Automated Metal Cleanliness Analyzer (AMCA) – An Alternative Assessment of Metal Cleanliness in Aluminum Melts

Hannes Zedel[1], Robert Fritzsch[1], Shahid Akhtar[2] and Ragnhild E. Aune[1]

[1] Dept. of Materials Science and Engineering, Norwegian University of Science and Technology (NTNU), Trondheim, NORWAY
[2] Hydro Aluminium, Karmøy Primary Production, Håvik, NORWAY

Communicating author: Hannes Zedel (hannes.zedel@ntnu.no)

The established industry standards for assessing the cleanliness of aluminum melts today are PoDFA (Porous Disc Filtration Apparatus) and LiMCA (Liquid Metal Cleanliness Analyzer) analyses. PoDFA yields good quality results and provides the necessary differentiation between inclusions but is slow and subject to human biases. LiMCA provides real time data without sufficient differentiation, limiting its usefulness for metal quality and process control. Complementary solutions are in demand that can provide similar quality results as PoDFA at the speed of LiMCA.

With the Automated Metal Cleanliness Analyzer (AMCA) an alternative solution is suggested that combines the strengths of both established approaches by standardized on-site sampling and automated image analysis for real time quality control. The present study shows a validation of the image analysis method by replicating the main cleanliness indicator of PoDFA in real industry samples at high precision.

Key words - Digital image processing, automated image processing, particle counting, metal cleanliness, quantitative stereology, PoDFA

1. Introduction

The assessment of the cleanliness of aluminum melts is critical for the aluminum industry both for quality control and process control and is defined by the amount of inclusions (indigenous and/or exogenous particulates) that are present in the molten metal [1]. Depending on the size of the inclusions, i.e. single large inclusions or a high number of small inclusions, they can negatively affect the mechanical and chemical properties of the end product and thereby jeopardize the quality of the cast.

Over the years, different techniques have been developed to evaluate the size and size distribution of the inclusions present in molten aluminum, as well as their shape and overall geometry. LiMCA (Liquid Metal Cleanliness Analyzer) represents the state of the art and allows for the counting of particulates in-situ prior to casting [2]. This approach can, however, not distinguish between gaseous-, liquid- and solid inclusions, and it also lacks the ability to distinguish between agglomerates, clusters or folded biofilms, which alters the particle count and can lead to errors in cleanliness characterization. Furthermore, detection of inclusions is limited to spherical diameters > 10 µm.

The other established method for deriving detailed analyses of sample contamination and inclusions in aluminum melt is the PoDFA (Porous Disc Filtration Apparatus)[3]. While the results of PoDFA analyses meet industry demands, the approach require melt samples to be processed manually by an operator subjecting the results to human biases. As a result, PoDFA analyses are time-consuming and therefore not suitable for on-site control of ongoing processes activities. The approach does, however, yield good quality results and provides the necessary qualitative and quantitative differentiation between the present inclusions.

With the Automated Metal Cleanliness Analyzer (AMCA), we suggest a viable alternative intended to produce metal cleanliness assessments at a similar level of detail as PoDFA during ongoing casts. AMCA is currently in development and is envisioned to feature integrated on-site hardware for standardized automated sample acquisition as well as automated digital image processing for generating metal cleanliness assessments in short time frames for real-time process control. AMCA is also conceptualized to establish itself as an alternative industry standard for quality control.

The purpose of the present study is to validate the image processing method by applying it to real industry PoDFA samples and quantitatively comparing AMCA's image processing results to the associated PoDFA report, generating a similar cleanliness indicator.

2. Method

2.1. Equipment and materials

For this study, 21 polished PoDFA samples and the associated PoDFA were provided by Norsk Hydro ASA, Karmøy, Norway. According to the report, the main metal cleanliness indicator is the total particle area in square millimeter per kilogram (mm^2/kg), classifying inclusion contamination as defined in Table 1.

Table 1: PoDFA inclusion classification[4]

Classification	**Inclusion content [mm^2/kg]**
(1) Very Light	0.0 – 0.05
(2) Light	0.05 – 0.1
(3) Moderate	0.1 – 0.4
(4) Heavy	0.4 – 1.2
(5) Excessive	≥ 1.2

During PoDFA analyses, micrographs of the filter cake are investigated by a semi-manual or manual grid classification method, allocating entire or partial grid squares to target classes of common inclusion types (see Figure 1). The target inclusion classes in the present PoDFA report cover (i) titanium diboride / titanium-rich inclusions, (ii) mixed oxides, (iii) anodic oxides, and (iv) carbides.

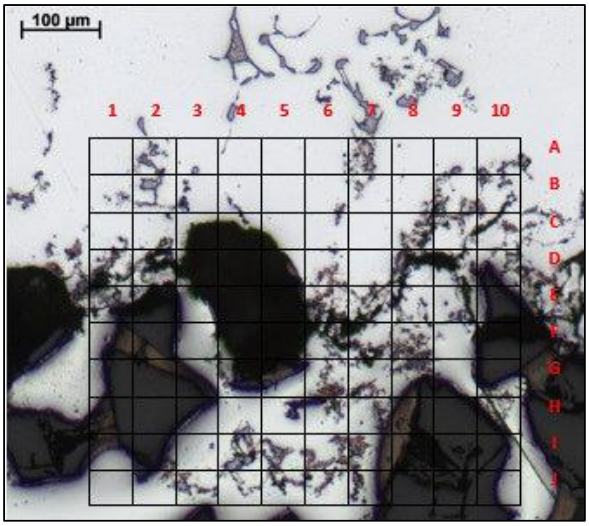

1	2	3	4	5	6	7	8	9	10	
	0.1				0.1	0.5			0.1	A
0.2	0.1	0.2	0.1		0.1	0.3	0.1	0.4	0.3	B
	0.1				0.2		0.6	0.4	0.2	C
0.3	0.2				0.2	0.1	0.1	0.1	0.3	D
0.4	0.2				0.5	0.3	0.1	0.3		E
					0.3	0.2	0.5	0.1		F
			0.2		0.4	0.2	0.6			G
				0.1	0.3	0.2	0.4		0.1	H
			0.1	0.1	0.5	0.3				I
		0.1	0.1	0.2	0.2					J

Figure 1: Typical grid classification approach in PoDFA analyses[5]

We captured micrographs of the filter cakes of the provided PoDFA samples at 100x magnification via optical microscopy, resulting in 14-16 images per sample, or 304 images in total for 21 PoDFA samples. To ensure statistical comparability, the images were taken with the same illumination settings of the optical microscope, adjusting only the sensor position and sharpness (to account for sample topology) between image captures.

2.2. Image processing

All micrographs were processed in Matlab 2019b[6], adapting and extending an algorithm previously used to quantify the size distribution of inclusions in solidified aluminum melts[7]. The deterministic image processing method utilizes gray scale intensity thresholds as well as various filters before and after thresholding to segment different types of objects in the micrographs targeting the classification of the following groups objects: (i) the filter, (ii) the bulk material/surface, (iii) titanium diboride / titanium-rich inclusions, (iv) mixed oxides, and (v) carbides.

For the purpose of this study, the classes were chosen to be similar to the PoDFA classes (see section 2.1) to allow meaningful comparisons. Depending on the image capturing technique and sample types, different classifications are possible and may allow for a more detailed composition differentiation in future applications of the method.

A general premise to the present approach is the Law of Large Numbers (LNN)[8], which indicates that with a larger numbers of micrographs the statistical results converge closer towards the expected results. In other words, the impact of a systematic error on relative comparisons is less if more samples are considered. With a higher number of micrographs, relative comparisons are therefore more statistically secured while absolute quantifications incorporate a stable quantifiable offset from the systematic error. Thereby, the suggested approach is especially suited for relative comparisons, e.g. answering the practical question which material has better quality than another.

The classification during image processing is performed at pixel precision and applies a hierarchical order: Easier targets get identified first to facilitate subsequent segmentations: filter → titanium rich inclusions → carbides → mixed oxides → sample surface. Figure 2 shows an example segmentation of one of the filter cake PoDFA samples.

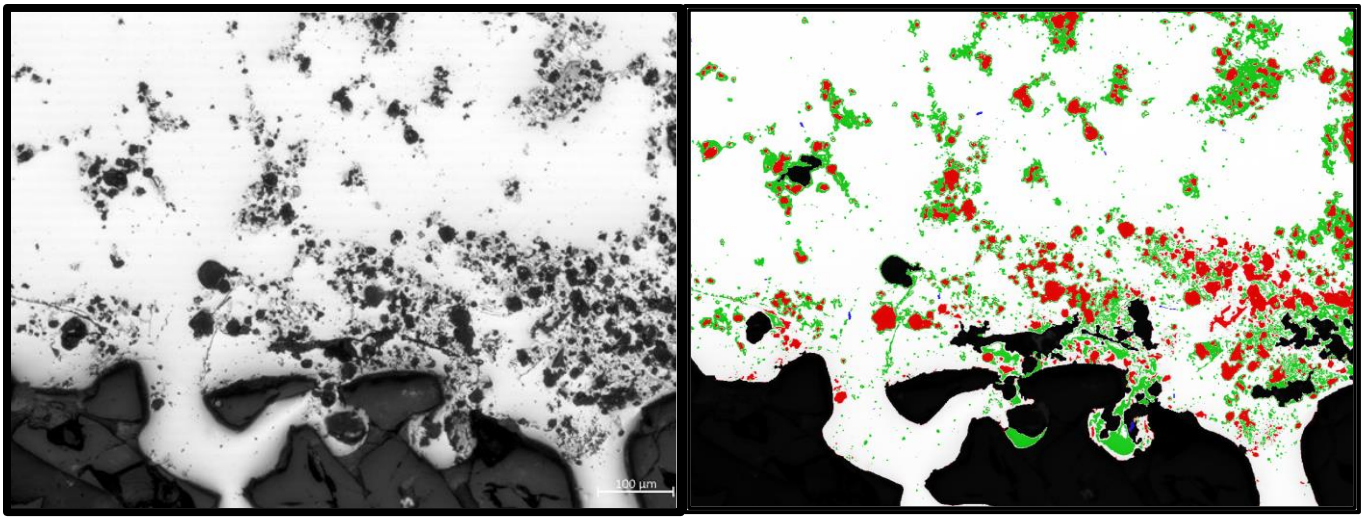

Figure 2: Example segmentation of a PoDFA sample; Color code: black=filter, red=titanium-rich inclusions, blue=carbides, green=mixed oxides, and white=surface; black and white printed shade code: black=filter, dark gray=titanium-rich inclusions, dark gray=carbides (low occurrence), light gray=mixed oxides, and white=surface

The following section provides an overview of the class-specific cues beyond the basic gray scale intensity range that were used to identify each class:

- Filter
  Filter parts were expected to be large (applying a size threshold) and often positioned at the edge of the bottom half of the PoDFA filter cake micrographs. Furthermore, the filter typically consists of solid parts without any small holes like pores, so artifacts can be removed by a filling function for enclosed islands.
- Titanium-rich inclusions
  Due to partial overlap of the gray scale intensity ranges of the titanium phase and the filter, a size threshold was applied to consider very large objects as part of the filter rather than the titanium phase. Objects at the edge of the micrograph may be filter parts as well and were processed by an adjusted size threshold. To account for artifacts like sample preparation scratches, shadows, or falsely identified carbides in this phase, a shape metric was applied: A low minor to major axis ratio threshold excluded objects from the titanium phase.

- Carbides
  Figure 3 illustrates carbide identification. Since the gray scale intensity range of carbides appeared to cover almost the entire spectrum from dark to light, this segmentation relied on a narrow size range and a strict shape metric (low minor to major axis ratio), leading carbides to be identified as long-shaped small objects.

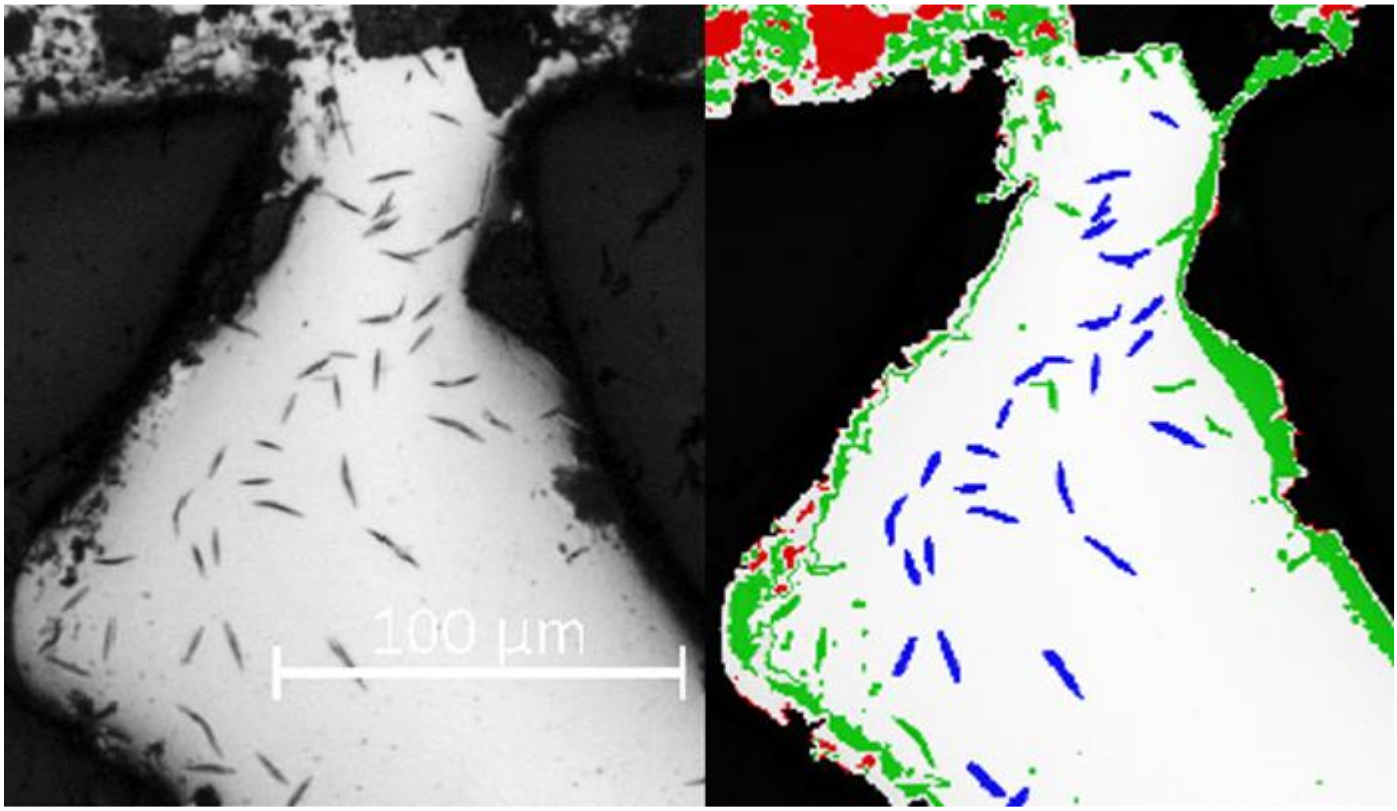

Figure 3: Example of carbide identification (blue / dark gray stick-shaped) in a PoDFA sample by the AMCA method.

- Mixed oxides
  The mixed oxides class grayscale intensity range showed to be overlapping with the gray scale intensity of topographical shadows (see Figure 4-1, compare to Figure 2). The algorithm treats adjacent pixels as singular objects, meaning that removing the false-positive shadows would also remove the target inclusions in that phase. To allow better differentiation, this phase was subdivided into three gray scale intensity ranges (see Figure 4-2) that then can be processed by size thresholds and shape metrics. This resulted in a drastic reduction of false-positive artifacts while maintaining the target objects (see Figure 4-3).

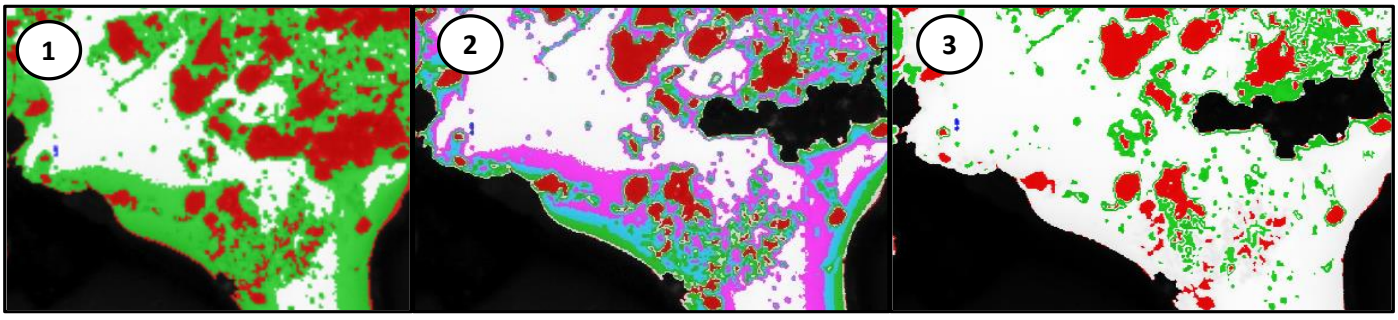

Figure 4: Example of artifact reduction by 3-layer differentiation of the mixed oxide class, enlargement of Figure 2

- Sample surface
  Due to the hierarchical segmentation approach, anything that was not allocated to any other class can be accounted for as the surface/bulk material.

To ensure the results' statistical comparability and to minimize human biases, the filters and filter settings of the algorithm are tuned to a few random micrographs and the settings are then blindly applied to all other images acquired by the same image acquisition method. This also allows for processing any number of acquired micrographs without an operator working on every image.

3. Results

For all of the 304 images, a classification of the entire micrograph into the five classes introduced in section 2.2 was derived by applying the AMCA image processing method. This included a pixel count for every target class, being equivalent to a percentage or an area in square micrometers. A size distribution for each inclusion type can generally be derived, however, was not relevant in the scope of the present study.

In PoDFA analyses it is common practice that the micrographs of the filter cake are assumed to be representative of the entire sample and that the total particle area is simply the sum of particles found in the filter cake micrographs (i.e. the sum of titanium-rich inclusions, mixed oxides, and carbides). It should be noted that in the present study, both the PoDFA and AMCA approaches ignored any inclusions distant from the filter cake. A direct comparison between the reported PoDFA results and the AMCA analysis is given in Figure 5.

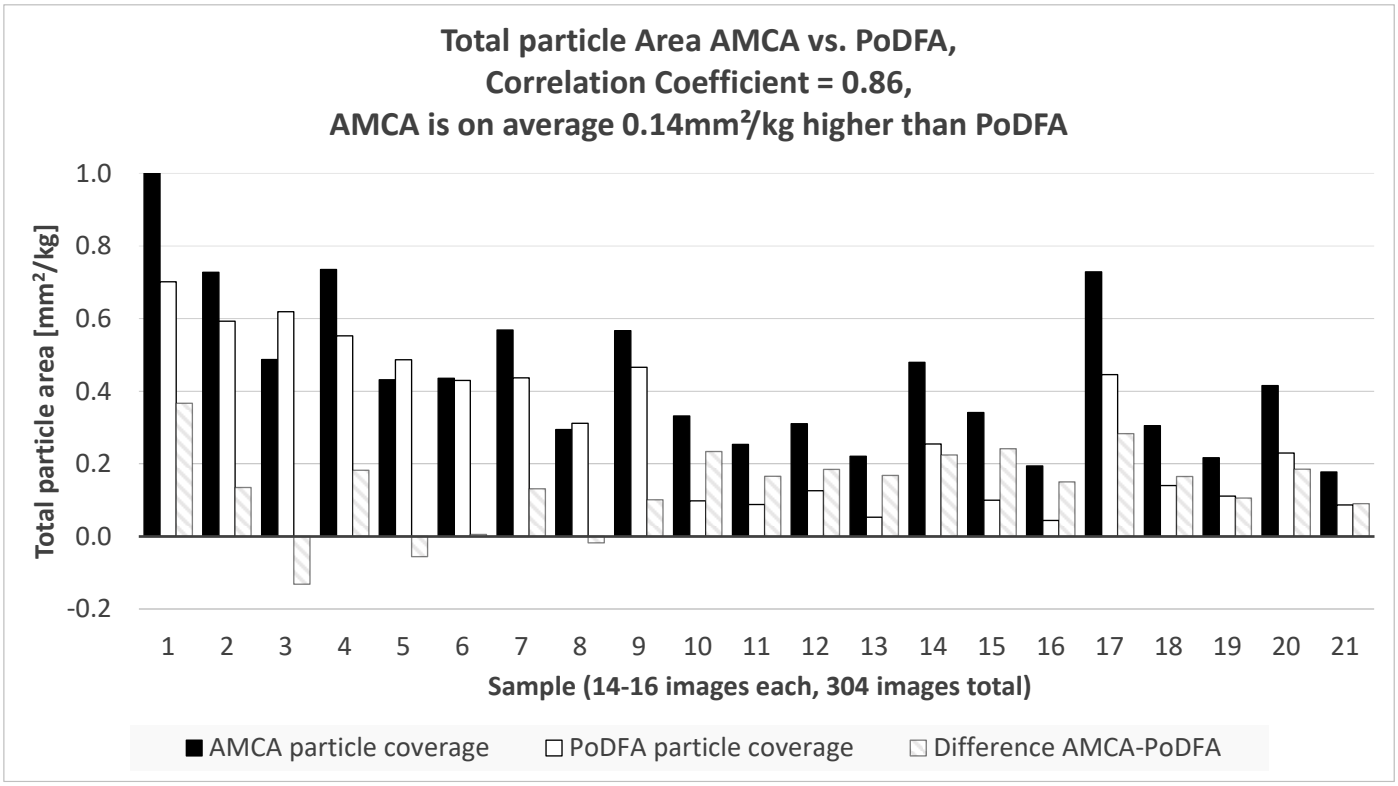

Figure 5: Comparison of the main metal cleanliness indicator (total particle area) in AMCA (black) and PoDFA (white) with a display of the difference between the data points (striped).

As can be seen in the figure, AMCA and PoDFA data are in the same order of magnitude and strongly correlated (r=0.86). The AMCA results show a positive offset of 0.14mm²/kg on average in comparison to the PoDFA data.

The time requirements for non-automated AMCA image acquisition and image processing in this study were as follows:

- Image acquisition (manual):
  - 5 minutes for setting up the microscope and sample
  - 10 seconds per image captured, or up to 3 minutes per sample
- Image processing:
  - 30 minutes (manual) for data handling and setting up the algorithm for a batch of images acquired by the same image acquisition setup
  - 3 seconds (automated) per micrograph or up to a minute per PoDFA sample

For a batch of 304 images covering 21 PoDFA samples, a total analysis time, including image acquisition from prepared samples and image processing, of less than three hours was required.

4. Discussion

It should be noted that the target classes of the AMCA and PoDFA approaches are not necessarily congruent as both rely on the interpretation of data from optical imaging. For the purpose of the present study, the classes of AMCA and PoDFA were assumed to be reasonably comparable. It should also be noted that neither AMCA nor PoDFA classes are proven to represent the real inclusions, meaning that deviations of AMCA results from PoDFA data do not necessarily mean that AMCA results are also deviating from real inclusions. The available data does not allow to derive any conclusions about whether AMCA or PoDFA data were closer to real inclusions. The validation compared to real inclusions requires more sophisticated methods and is scheduled for future work.

As presented in Figure 5, there is a positive offset of AMCA data compared to PoDFA data, indicating a systematic overestimation of the total particle area. There are several factors likely to contribute to that offset:

- Despite removing the majority of the residual false-positive artifacts from topographical shadows, as exemplified in Figure 4, there were still some left.
- There was a general bias by the image acquisition during AMCA analyses as it is arbitrary how much of the filter is included in the images. Our images contained inclusions within the filter that are usually not accounted for in PoDFA analyses but are counted in the AMCA Matlab algorithm. An example of that overestimation is provided in Figure 6 by the highlighted box at the bottom right.
- Compared to real counts, there might have been an underestimation by the PoDFA analyses due to the grid classification and associated human biases (see Figure 1).

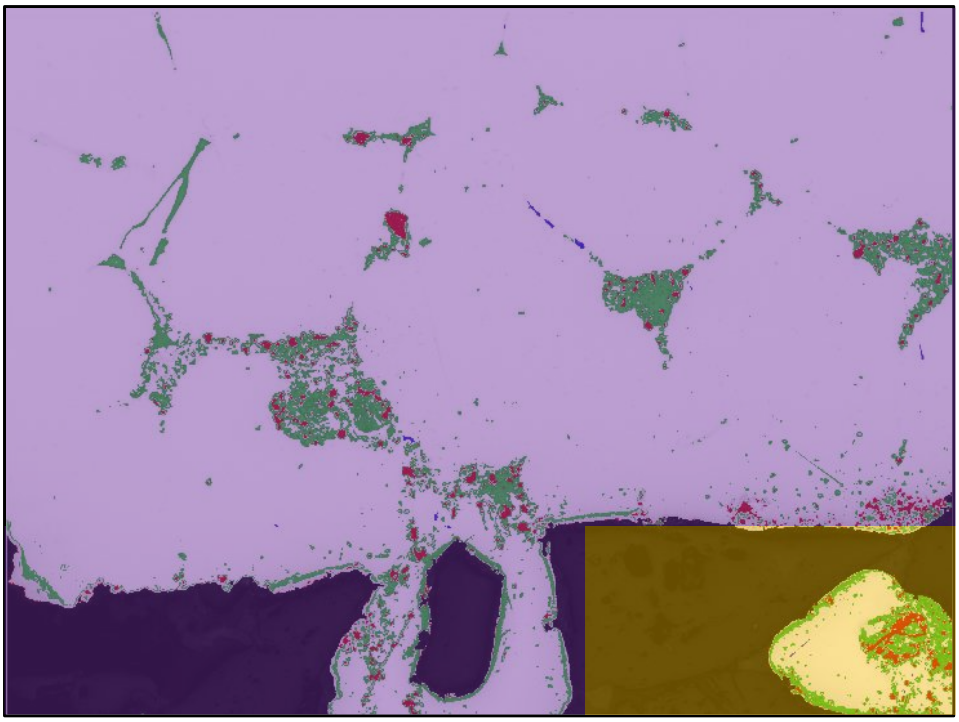

Figure 6: Example of AMCA scope exceeding PoDFA scope by including particles inside the filter (yellow/highlighted box at the bottom right) in addition to the filter cake (purple, typical PoDFA scope)

The resulting strong correlation between the PoDFA data and the AMCA results conveys two major implications:

- As expected, the offset is non-linear, meaning it is not a stable offset per image but an offset scaling with the total particle area. The more inclusions there are in an image, the greater the absolute deviation between PoDFA and AMCA data will be. This suggests that a metal cleanliness indicator based on AMCA data should use an adjusted non-linear classification of cleanliness levels slightly higher than the PoDFA classifications shown in Table 1.
- Despite the deviations between both data sets, the AMCA result is about as meaningful as the PoDFA data in view of assessing the metal cleanliness of molten aluminum, making it a viable alternative.

Furthermore, the aluminum industry representatives stress the increasing importance of quantifying carbide contents in aluminum melts, as their impact on metal quality has become more apparent in recent years. To the knowledge of the present authors, there is

no other method that identifies carbides with a similar precision as the AMCA image processing method (see Figure 3). Therefore, AMCA might uniquely meet related market demands.

5. Conclusion

The aim of the present study has been to validate the AMCA image processing method by deriving particle inclusion data from real industry PoDFA samples and deriving a metal cleanliness classification similarly meaningful as the PoDFA report data. The obtained AMCA results strongly correlate with the available PoDFA data, suggesting that the derived AMCA data is similarly meaningful for assessing metal cleanliness. A slight positive offset was identified in comparison to the PoDFA data, which expectedly scales with the level of sample contamination.

Notably, the AMCA image processing method is minimalistic in resources, as the manual operator time and associated labor costs do not scale with the number of samples – rather, the operator sets up the algorithm for a batch of images that was acquired under the same conditions, letting the algorithm process any number of samples automatically. Therefore, AMCA is likely to be faster and cheaper than established approaches that provide similar results.

In the context of recently increasing industry interest in carbide quantification, AMCA may have a unique position of being able to provide high precision carbide identification from micrographs that established methods cannot provide to this date.

6. Future Work

This study served as a validation of the image processing method, proving that it can produce results similarly meaningful as PoDFA data for assessing metal cleanliness of aluminum melt when being applied to PoDFA samples. The next step is to assess how closely AMCA can match real inclusions by assessing either known contaminations or using material-specific quantitative methods for further benchmarking. AMCA is intended to develop into an autonomous industry level solution by incorporating the image processing method into innovative equipment to automate sample and image acquisition from ongoing processes. By standardization of the sample and image acquisition steps, the image processing can be automatized, further improving its precision. The prospected solution is envisioned to serve as an integrated system for inhouse process control and an alternative metal cleanliness standard for the aluminum industry.

Furthermore, we aim to challenge the established assumption that the filter cake contamination is representative for the entire sample by quantifying inclusions on the entire sample surface.

7. Acknowledgment

The authors wish to express their gratitude to the Department of Materials Science and Engineering and the Department of Chemistry at the Norwegian University of Science and Technology (NTNU) for the intensive usage of the optical equipment in the microscopic laboratory, to NTNU Technology Transfer AS (NTNU TTO) for their administrative and strategical support of the project, as well as to Norsk Hydro ASA in Karmøy for the provision of PoDFA samples and continuous support of the project.

REFERENCES

[1] D. Doutre, B. Gariépy, J. P. Martin, and G. Dubé, ‘Aluminium Cleanliness Monitoring: Methods and Applications in Process Development and Quality Control’, in *Essential Readings in Light Metals*, J. F. Grandfield and D. G. Eskin, Eds. Cham: Springer International Publishing, 2016, pp. 296–304.

[2] R. Guthrie and M. Li, ‘In Situ detection of inclusions in liquid metals: Part II. Metallurgical applications of LiMCA systems’, in *Metallurgical and Materials Transactions B*, vol. 32, 2001, pp. 1081–1093.

[3] ABB Inc., ‘PoDFA, The complete solution for inclusion measurement, Inclusion identification and quantification analysis’. 2016, [Online]. Available: https://library.e.abb.com/public/b706913462934969befe277d80880795/PB_PoDFA-EN_A.pdf.

[4] C. Stanica and P. Moldovan, ‘Aluminium melt cleanliness performance evaluation using PoDFA (Porous Disk Filtration Apparatus) technology’, *UPB Sci Bull Ser. B*, vol. Vol. 71, no. Iss. 4, 2009, [Online]. Available: https://www.scientificbulletin.upb.ro/rev_docs_arhiva/full6739.pdf.

[5] P. V. Evans, P. G. Enright, and R. A. Ricks, ‘Molten Metal Cleanliness: Recent Developments to Improve Measurement Reliability’, in *Light Metals 2018*, O. Martin, Ed. Cham: Springer International Publishing, 2018, pp. 839–846.

[6] *MATLAB (2019)*. Natick, Massachusetts: The MathWorks Inc.

[7] H. Zedel, R. Fritzsch, S. Akhtar, and R. E. Aune, ‘Estimation of Aluminum Melt Filtration Efficiency Using Automated Image Acquisition and Processing’, in *Light Metals 2019*, C. Chesonis, Ed. Cham: Springer International Publishing, 2019, pp. 1113–1120.

[8] N. Etemadi, ‘An elementary proof of the strong law of large numbers’, *Z. Für Wahrscheinlichkeitstheorie Verwandte Geb.*, vol. 55, no. 1, pp. 119–122, Feb. 1981, doi: 10.1007/BF01013465.